INVESTIGATION OF THREE BLADED HORIZONTAL AXIS WIND TURBINE USING BEM THEORY

Prasanta Raut[1], Uttam Timalsina[2], Ramesh Kumar A[3]

[1,2] *Mechanical Engineering, Sona College of Technology, Salem-636005, Tamilnadu, India*
[3]*Assistant Professor, Department of Mechanical Engineering, Sona College of Technology, Tamilnadu, India*

---***---

Abstract - *Modern wind turbines require specially designed turbine blades to extract much of the energy from the wind. The blades can be imagined as an extension of a 2D airfoil cross section whose thickness reduces as it extends along the tip. There are several popular ways of designing wind turbine blades such as Vortex Lattice (VL) method, Reynolds averaged Navier Stokes method and Blade Element Momentum (BEM) theory method. In this research, BEM theory method has been used to design wind turbine blades for operating at a class III region located in a remote district of Nepal. A statistical analysis of wind speed and power density of the region based on Rayleigh and Weibull models have been successfully carried out* [1]. *The place has been identified as an excellent source of wind with little roughness factor (0.143) and year around blowing wind. However, the region lacks electricity like most of the remote locations in the country. So an attempt has been made to conceptualize the possibility of wind power plants in the region by designing various wind turbine blades and analyzing them under aerodynamic loading conditions using the blade element momentum theory method.*

*Key Words***: Airfoil, NREL, NACA, XFOIL, axial force, axial induction factor, chord, twist angle, vortex, wake, inviscid.**

1. INTRODUCTION:

Nepal has a total installed capacity of 5100.11 GWh as of the end of 2017. As per the report, Nepal requires 7338.41 GWh by 2020, 12242.23 GWh by 2025, 18481.66GWh by 2030 and 26819.22GWh by 3013 @ 4.5% economic growth scenario[2]. Though Nepal has a large potential for the hydropower production, its exploitation has been to a very minimal, and therefore, a significant amount of energy supply has to come from other sources. However, the use of solar energy has been increasing in the country; the wind is a good source of renewable power with the generation capacity of 3000 MW which is far more greater than the electricity demand of Nepal.[3]

As a result of the following reasons to utilize the wind energy essential:

- Carbon dioxide content is rising in the atmosphere during the last decade 390-400ppm in the span of 2011 to 2016. CO_2 concentration was averaged to 418.44 ppm on July 2016 and wind turbine provides energy with a zero emission of carbon.[4]

- Global temperature is also rising during the last century; the rise of 1.5 degree Celsius is seen in the recent years.[5]

- Wind energy is cost competitive.

- They can provide a large number of employment opportunities to the locals.

- They can be installed fast with respect to the hydropower which is one of the great sources of electricity in Nepal.

- This can also be economical when large blades are used.

According to the exact worldwide statistics, the global wind power cumulative capacity can be shown as below:[6]
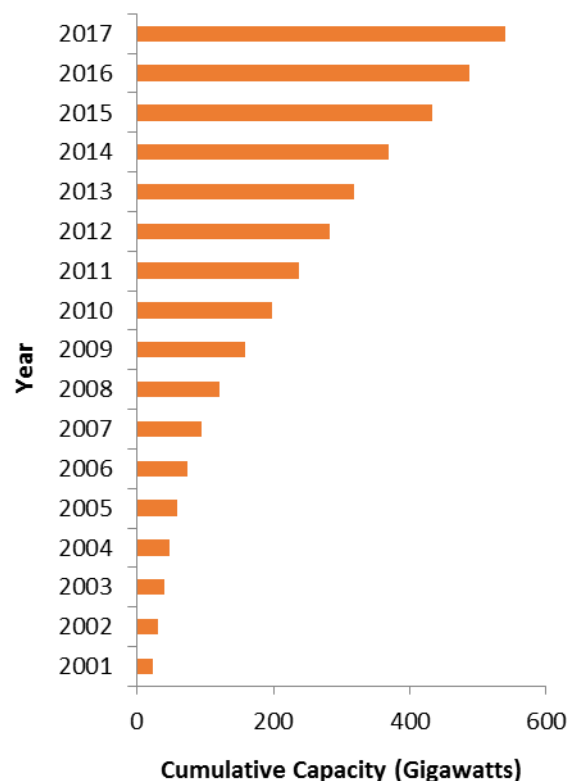

Fig-1: Global wind power cumulative capacity

From the Fig-1, it can be concluded that the amount of electricity generated is doubling about every three years.

The generated electricity is used in a variety of electricity demands, from lighting houses in the suburbs to cutting-edge technology industries.

2. Working Principle

For the purpose of the wind turbine, a symmetric airfoil is considered which is attacked at the leading edge by velocity (w) at an angle of attack (α) no lift occurs but only drag. As the angle of attack increases gradually from 0, a positive lift force is generated this is proportional to the area of the blade and to the square of the velocity.

Mathematically, lift force and drag force can be determined as:

$$Lift\ force\ (L) = \frac{C_L(\alpha)\rho}{2} w^2 (bc)$$

$$Drag\ force\ (D) = \frac{C_D(\alpha)\rho}{2} w^2 (bc)$$

The lift coefficient (C_L) and drag coefficient (C_D) are determined by means of wind tunnel experiments on the respective airfoils.

3. Blade Element Momentum Theory (BEM)

The designing of the blade using BEM theory which is the combination of blade element as well as blade momentum theory. With an aim for determining thrust as well as the moment force which were caused by the fluid in each of the blade elements, BEM calculation was done.

3.1 Blade Element Theory

The first one to propose the blade element theory was Dr Zwiecki in the 1890s to analyze the aeroplane propeller. This theory is based on the assumption that each blade section acts as a 2D airfoil for producing the aerodynamic forces. Each blade is split into certain elements for which different flow occurs in each element.[7] This results in different speed, length of the chord, twist angle, induction factors and other properties. The contribution from each blade element is added to give the final performance. The BEM theory relies on two major assumptions which are:[8]

- Aerodynamics interactions between different blade elements are not considered.
- The lift and drag coefficient are used for determining the forces on the blade element solely.

3.2 Blade Momentum Theory

This theory was developed more than a century ago for predicting the performance of the ship propellers. It is a fast and simple method to estimate the necessary power. It is also an efficient and sufficient tool to determine the size of the rotor. However, for a given power plant it is not enough to design the rotor using this theory alone. Momentum theory assumes a controlled volume whose boundaries are the surfaces of a stream tube and two cross-sections of the stream tube and the flow tends to happen only at the end of the tubes. Furthermore, the other assumptions used by this theory are:[8]

- Homogeneous, incompressible and steady-state fluid flow
- Absence of frictional drag
- Uniform thrust over the disc area
- Wake without rotation

4. Design Procedure

As one of the important tasks during the design of wind turbine is choosing an appropriate rotor size, require extracting the necessary amount of power from the wind. This also requires the proper selection of the site, i.e. the wind speeds is adequate enough for the power production. In this research, a class III site is chosen for the wind turbine for the production of 250 KW or 3500000 KWhr of power per year. The class was determined as defined by the International Electrotechnical Commission (IEC) standard which can be shown in below table 1:[9]

Table-1: Wind class according to IEC

Table class	IEC I High wind	IEC II Medium wind	IEC III Low wind
Annual average wind speed	10m/s	8.5m/s	7.5m/s
Extreme 50 year gust	70m/s	59.5m/s	52.5m/s
Turbulences classes	A 18% B 16%	A 18% B 16%	A 18% B 16%

The chosen site lies in Jumla, a remote district in Northwestern Nepal. The lack of electricity facility in this region if national attention in the place seems to have got sufficient wind energy to sustain a 250KW wind turbine or even more. Various research has been done in the past focusing this place and its wind seed assessment, i.e. [1]. Jumla has an average wind speed of 6m/s at 10 meters from the ground. At the height of around 60 meters, the wind speed reaches up to 7.75m/s where the rotor can be attached to the hub. The wind speed at 60 meters is calculated by using an empirical power law model as shown below:

$$V_Z = U_H \left(\frac{Z}{H}\right)\alpha$$

Where,

V_Z = wind speed at height Z
U_H = reference height, 10 m in this case

H= required height for the wind speed

A= 0.143 (a constant which depends upon the surface roughness)

4.1 Losses in Rotor Design

The rotor is the heart of the wind turbine, and this paper aims to design and calculate the performance characteristics of the designed rotor. The first step in designing the rotor is to assess the power coefficient of the rotor and determining the diameter or radius of the rotor which is referred as the blade length. There is involvement of various losses that might occur in the ideal scenarios while calculating the power coefficient of the rotor. The various losses that were accounted were:

- Profile loss resulting from drag force which is ignored in the ideal case
- The losses resulting from the flow around the tip called tip losses
- Loss due to wake rotation downstream

4.1.1 Profile Loss:

Profile losses arise from the drag forces which are often ignored when designing an ideal blade. However, they need to be considered while designing any rotor which is supposed to work in a real-time environment. Profile loss was calculated by using the following formula as mentioned below for the calculation of optimum tip speed ratio.[10]

$$\eta_{Profile} = 1 - \left(\frac{\lambda_A}{\varepsilon}\right)$$

Where,

$\lambda_{Profile}$ = speed ratio

ε = drag coefficient ratio

4.1.2 Tip Loss:

Due to the flow of air around the tip of the blade, the tip loss occurs. For this loss to occur, air flows from the pressure side to the suction side and can be calculated as;

$$\eta_{tip} = 1 - \left\{\frac{1.84}{B\lambda_A}\right\}$$

For $\lambda_A > 2$ (B is the number of blades)

4.1.3 Wake Loss:

In the wind turbine, there is the presence of blade wake which contributes to loss of power coefficient. This research also accounts the wake rotation and its effect to calculate the losses for the rotor design. Table 2 value was used to calculate the losses due to blade wake rotation.[10]

Table-2: Calculating the losses due to blade wake rotation

Tip Speed Ratio (TSR)	$CP_{schmitz}$
0.5	0.238
1	0.4
1.5	0.475
2	0.515
2.5	0.531
3	0.537
3.5	0.538
4	0.541
4.5	0.544
5	0.547
5.5	0.55
6	0.553
6.5	0.556
7	0.559
7.5	0.562
8	0.565
8.5	0.568
9	0.57
9.5	0.572
10	0.574

4.2 Calculation of power coefficient:

Having calculated all the losses, the actual power coefficient C_P is calculated by the sum of profile loss, tip loss and the wake loss.

$$C_P = \eta_{Profile} + \eta_{tip} + CP_{schmitz}$$

The power coefficient determines the quality of design, i.e. higher the power coefficient better is the design. But in some cases, optimum tip speed ratio should be chosen as higher tip speed ratio might result in more loads to the rotor root.

4.3 Calculation of Rotor Radius:

We calculated the rotor radius by using the below-mentioned expression which related the power required to produce with wind characteristics and rotor radius and power coefficient as;

$$R = C_P \eta \frac{1}{2} \rho \pi R^2 V^3$$

Where,

R= rotor radius

η= electrical and mechanical efficiency, usually 0.9

ρ= air density

V= wind velocity

This equation relates the power required to produce with wind characteristics and rotor blade radius and the power coefficient.

4.4 Selection of Optimum TSR

For the selection of optimum tip speed ratio, considering all the losses for determining the power coefficient. The losses were dependent on TSR, C_L-C_D ratio and the number of blades. As the designed TSR raise the power coefficient rises up to a certain level, then the power coefficient starts decreasing. By considering the best power coefficient, the corresponding TSR was chosen as the optimum TSR. In some cases, the TSR increases while the power coefficient seems to rise continuously for which the TSR was used below 9. This was because the interfering aerodynamic noise increases approximately with the fifth power of the blade tip speed ratio.[11]

4.5 Number of Blades:

We chose the number of the blade as 3 for this design work as it possesses the following benefits as compared to the others, i.e., 1,2, and 4 bladed turbines;

- They are more efficient than one or two-bladed turbines.
- They are more cost-effective than the four-bladed turbines.
- Aesthetically they are more appealing.

4.6 Selection of Airfoil/s:

A wind turbine blade can be composed of a single airfoil along the span or a variety of airfoil along the span. Here in this research, we designed the blade which consisted of a single airfoil of NACA 4415 series along with its span and its performance characteristics, as well as load behaviour, is calculated.

4.7 Blade chord:

One of the important blade geometry parameters is the blade chord, which is the length of an imaginary line joining the leading and the trailing edge of the airfoil. The following formula to calculate the optimum blade chord length.

$$Chord\ (C) = 2\pi R \frac{1}{Z} \frac{8}{9C_L} \frac{1}{\lambda_D \sqrt{\lambda_{D^2} \left(\frac{r}{R}\right)^2 + \frac{4}{9}}}$$

4.8 Iterative Procedure:

We followed an iterative procedure to calculate the relative flow angle, axial induction factors and angular induction factors as it could not be derived from the single equation and a single step. A single step was done first to guess their initial values, and then the iteration was begun until they converged to a near equal value of some tolerance. The initial guesses of the iteration are provided by the following equations:[8]

$$\beta = 90° - \frac{2}{3}\tan^{-1}\left(\frac{1}{\lambda_r}\right)$$

After the value of β is calculated, the initial value of the angular induction factor is given by;

$$a = \left(1 + \frac{4cos^2\beta}{\sigma C_L sin\beta}\right)^{-1}$$

Then the angular induction factor is estimated by using the equation given below:

$$a' = \frac{1 - 3a}{4a - 1}$$

After the initial guesses are made, the iterative procedure follows different equations.

$$tan\beta = \frac{\lambda_r(1 + a')}{(1 - a)}$$

The value of β was calculated from the above equation after substituting the initial guesses of a and a′. Then from the following equation, value of 'a' is calculated by substituting the values of β and corresponding life coefficient C_L.

$$\frac{a}{1 - a} = \frac{\sigma'(C_L sin\beta)}{4cos^2\beta}$$

The value of β and a is then substituted in the following equation which yields the angular induction factor

$$\frac{a'}{1 - a} = \frac{\sigma'C_L}{4\lambda_r cos\beta}$$

The iteration was carried until the two consecutive values of a and a′ converged with some minimal tolerances. The algorithm for the iteration can be formulated as follows:

Step 1: Guess β and initial values of a and a′

Step 2: Using the a and a′ value, calculate β again

Step 3: Using β calculate a again

Step 4: using a calculate a′ again

Step 5: Compare the initial and final values and repeat step 1.

4.9 Calculation of twist angle:

The twist angle can be defined as the angle at which the blade section is twisted to compensate the change in relative velocity along the blade. The twist angle θ was calculated after finding the values of relative flow angle and angle of attack. On selecting the required airfoils and analyzing them in XFOIL feature in Qblade software, the optimum angle of attack can be known. The relation for the angle of attack can be shown as,

$$Angle\ of\ attack\ (\alpha) = \gamma - \beta$$

After knowing these parameters, we designed the blades in Qblade and performed various simulations.

5. Design

5.1 Blade Design:

The blade design consisting of single airfoil along its span. The airfoil used is the NACA4415 which has been evaluated by Cetin et al. for its optimum tip speed ratio. Table 3 shows the selection of tip speed ratio:

Table-3: Selection of tip speed ratio

TSR	$CP_{schmitz}$	$C_L \backslash C_D$	Profile Loss	End Loss	C_p
0.5	0.238	129.065	0.996126	-0.22667	-0.05
1	0.4	129.065	0.992252	0.386667	0.15
1.5	0.475	129.065	0.988378	0.591111	0.27
2	0.515	129.065	0.984504	0.693333	0.35
2.5	0.531	129.065	0.98063	0.754667	0.39
3	0.537	129.065	0.976756	0.795556	0.41
3.5	0.538	129.065	0.972882	0.824762	0.43
4	0.541	129.065	0.969008	0.846667	0.44
4.5	0.544	129.065	0.965134	0.863704	0.45
5	0.547	129.065	0.96126	0.877333	0.46
5.5	0.55	129.065	0.957386	0.888485	0.46
6	0.553	129.065	0.953512	0.897778	0.47
6.5	0.556	129.065	0.949638	0.905641	0.47
7	0.559	129.065	0.945764	0.912381	0.47
7.5	0.562	129.065	0.94189	0.918222	0.48
8	0.565	129.065	0.938016	0.923333	0.48
8.5	0.568	129.065	0.934142	0.927843	0.49
9	0.57	129.065	0.930268	0.931852	0.49
9.5	0.572	129.065	0.926394	0.935439	0.49
10	0.574	129.065	0.92252	0.938667	0.49

From the above table, the power coefficient fairly stayed constant at the TSR of 8.5 and above after which the radius of the rotor was calculated.

After this, the relationship between angle of attack and lift and drag coefficient ratio was studied with the use of XFOIL which shown in Fig-2.
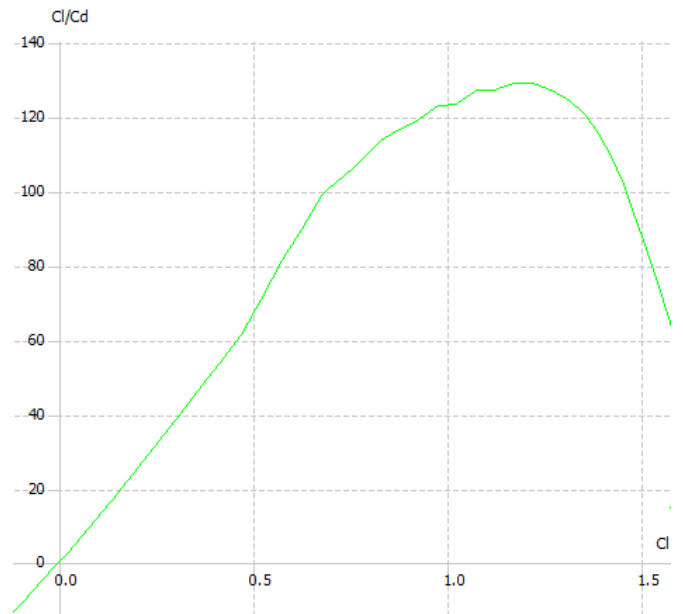

Fig-2: C_L-C_D ratio vs angle of attack for NACA 4415

After studying the airfoil characteristics, the design procedure began in Qblade. The maximum lift-drag coefficient ratio to be 128.665 at an angle of attack 7°. Different parameters such as blade position, blade chord and blade twist angle were fed into the software after the calculations, and the blade design was prepared. The designed result for the blade is shown in Fig-3.
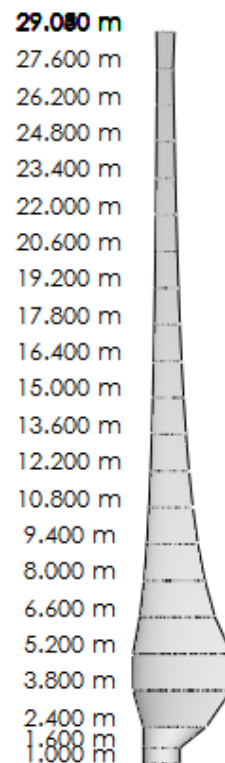

Fig-3: Blade design with the position

The program also allows choosing the number of blades as per the requirement. A three-bladed HWAT shown in Fig-4.
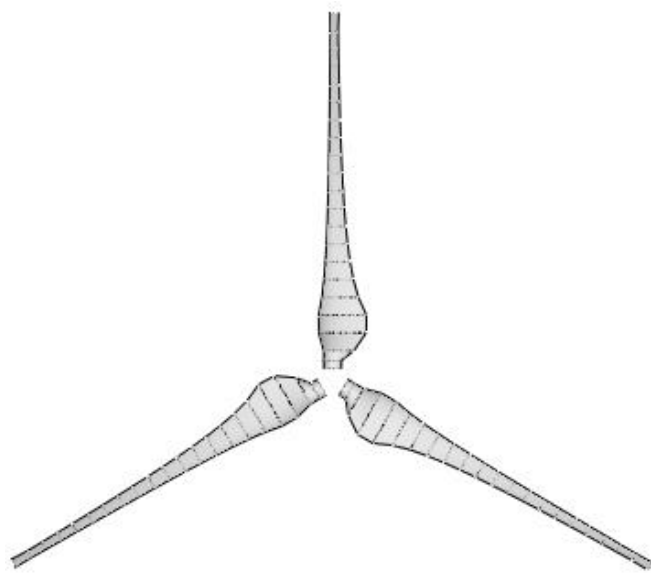

Fig-4: Three-bladed HAWT

5.2 Load Calculation:

After the design work, the forces exerted on the wind turbine blade were calculated with the use of BEM theory. Following equations were used for the load calculation:[8]

$$dF_x = \sigma'\pi\rho\frac{V^2(1-a)^2}{cos^2\beta}(C_L sin\beta + C_D cos\beta)rdr$$

$$dF_x = \sigma'\pi\rho\frac{V^2(1-a)^2}{cos^2\beta}(C_L cos\beta - C_D sin\beta)r^2 dr$$

$$dF_\theta = B\frac{1}{2}\rho W^2(C_L cos\beta - C_D sin\beta)cdr$$

The equations provide the axial force dF_x and torque dT acting on each blade element. The total torque was then calculated by summing up the forces and torque for the entire blade section. The table as in APPENDIX depicts the load exerted on the designed wind turbine blade.

6. Simulations

6.1 BEM Simulation:

BEM simulation of the turbine which confirms our finding regarding the load exerted on the blade. It allowed us to calculate the thrust, torque and different dimensionless characteristics coefficient. The coefficient of power thrust and torque were also calculated with the help of the BEM simulation tool. The relation between the power coefficient and TSR is shown in Fig-5.
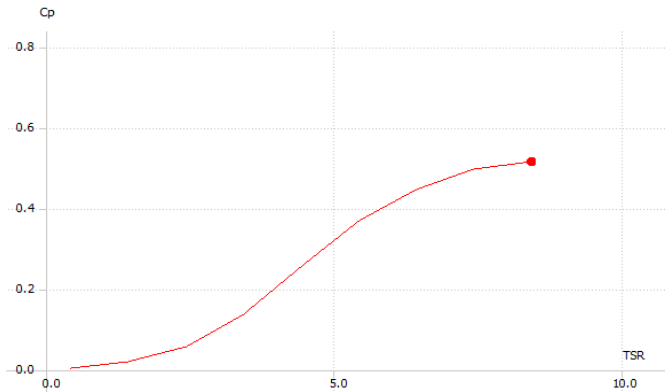

Fig-5: C_P vs TSR

The power coefficient from the simulation comes around 0.509 which was very near to the power coefficient that we calculated before the design which was 0.49. Thus it suggests our calculation and the simulation were in consistency with each other. Other relations such as thrust and torque exerted on the wind turbine rotor with the TSR can also be shown in Fig-6.
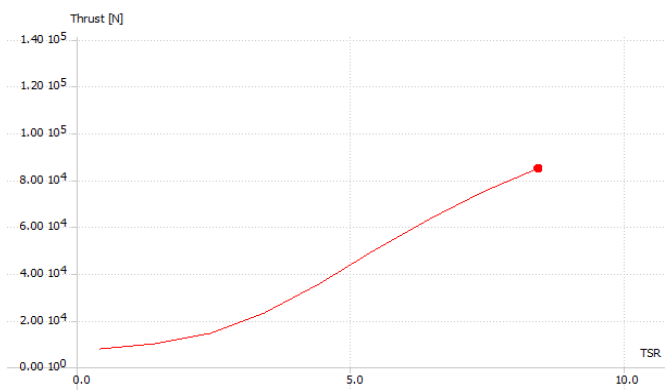

Fig-6: Thrust vs TSR

We can observe from the graph that the axial thrust exerted upon the rotor blade is around 85,000N which is close to our calculated load of 86,725N.
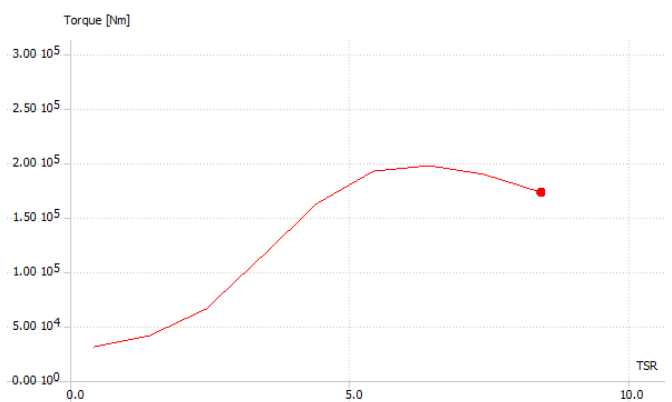

Fig-7: Torque vs TSR

From the Fig-7, we can see that the total torque exerted on the rotor blade is around 1.7×10^5 Nm which is near to our calculated torque for the rotor, i.e. 1.5×10^5 Nm.

6.2 Dimensionless characteristics Curve:

Dimensionless characteristics curves are the curves plotted between the coefficient of power, thrust and torque against the tip speed ratio. The power coefficient has already been plotted in the simulation outcomes section. The thrust and torque coefficients against the tip speed ratio which were plotted in Qblade are shown in Fig-8 and Fig-9.
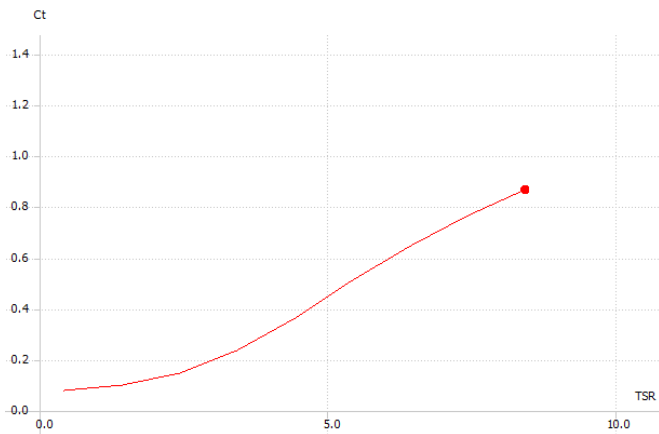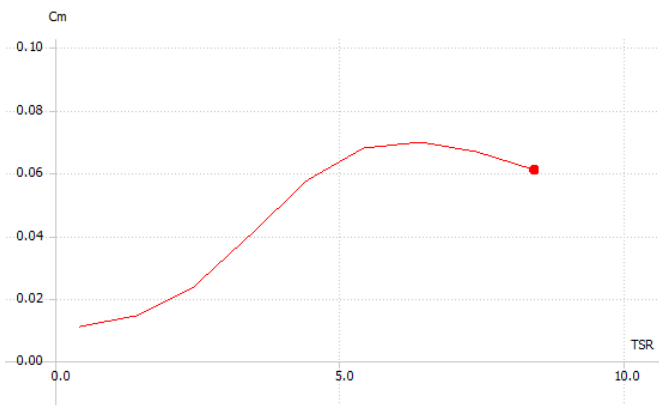

Fig-8: C_t vs TSR

Fig-9: C_m vs TSR

6.3 Load Behavior (Analysis):

Fig-10 shows the load and deflection test on the blade. The load analysis was carried out within Qblade using one of its tools called QFEM. Although not on par with sophisticated software like ANSYS, this tool provided an easy environment to perform the analysis. The material selection for the blades was made based on the recent convention of using carbon fibre in the shell and high-quality foam in the internal section to provide flexibility and to impart lightweight.
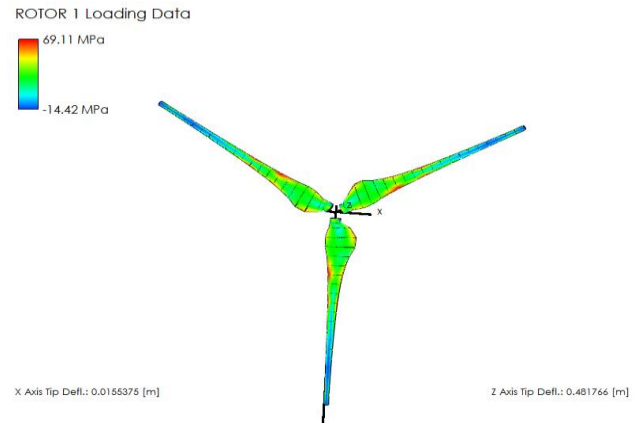

Fig-10: Load and deflection test on the blade

From the analysis, we can observe that the X-axis tip deflection is around 0.01553m while the Z-axis deflection is around 0.48m. This will cause the rotor blades to bend along the direction of wind causing stress in the portions marked red.

6.4 Nonlinear lifting line theory and simulation:

This method belongs to the family of "Vortex methods". In terms of computational cost, complexity and modelling of the physics, the vortex methods are situated in-between the blade momentum (BEM) theory and computational fluid dynamics (CFD). Vortex method can be used to model the flow field as an inviscid, incompressible and irrotational where the elements get introduced either in the straight and curved line segment.[12]

Some studies even show that the vortex methods are identified as suitable to replace BEM codes in the near future to achieve high accuracy in turbine design and certification applications. Beside that the vortex method also produces the unsteady velocity field around the rotor as well as a wake in every time step. The wind leaving the wind turbine is turbulent in nature and rotates in a corkscrew-like pattern which is called a wake. Wake can be determined by the environmental factors as well as the model of the wind turbine itself.[13] The result for the wake rotation of the rotor is shown below:
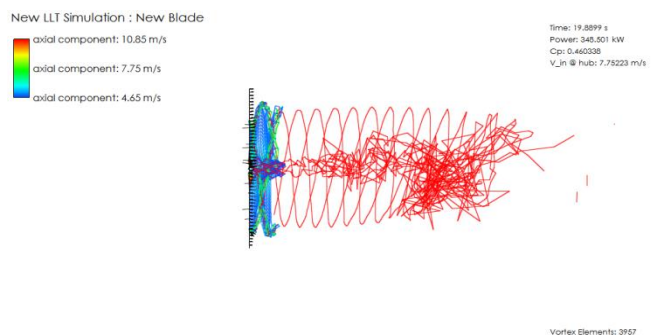

Fig-11: Wake rotation simulation of the rotor

In the Fig-11, we can see the wake forming at the left portion of the rotor. Also, the turbulence created in the air due to wake (scrambled portion) can be seen. Wake results in the turbulence in the air leaving the wind turbine blades and reduce the wind speed which might cause inefficiency in the rotor installed behind the corresponding turbine. However, the distance up to which the wake effect extends in still a matter of debate.

7. Conclusion

In a developing country like Nepal, there is no sufficient production of the electricity which results in the price hike. Moreover, in the remote places like Jumla, the chosen site, lacks electricity even in the modern days. This paper deals with the possibility of providing an adequate amount of energy to the remote location within low cost. Not only the electricity, but it also deals with providing the employment opportunities to the local people and utilizes the wind resource as a tool to reduce the threat of climate change.

REFERENCES

[1] A. Parajuli, "A Statistical Analysis of Wind Speed and Power Density Based on Weibull and Rayleigh Models EXPERIMENTAL VALIDATION View project A Statistical Analysis of Wind Speed and Power Density Based on Weibull and Rayleigh Models of Jumla , Nepal," no. August, 2016.

[2] E. Demand and F. Report, "Water and Energy Commission Secretariat Electricity Demand Forecast Report," no. January, 2017.

[3] A. Ragheb and M. Selig, "Multi-Element Airfoil Configurations for Wind Turbines," 29th AIAA Appl. Aerodyn. Conf., no. June, pp. 1–13, 2011.

[4] S. Nomura, H. Mukai, Y. Terao, T. Machida, and Y. Nojiri, "Six years of atmospheric CO_2 observations at Mt. Fuji recorded with a battery-powered measurement system," Atmos. Meas. Tech., vol. 10, no. 2, pp. 667–680, 2017.

[5] "Earth Flirts with a 1.5-Degree Celsius Global Warming Threshold - Scientific American." [Online]. Available: https://www.scientificamerican.com/article/earth-flirts-with-a-1-5-degree-celsius-global-warming-threshold1/. [Accessed: 18-Mar-2018].

[6] Global Wind Energy Council, "GLOBAL WIND STATISTICS 2017 Global Wind Energy Council," 2018.

[7] P. M. Cavcar, "Blade Element Theory," Aviation, pp. 1–5, 2004.

[8] G. Ingram, "Wind Turbine Blade Analysis using the Blade Element Momentum Method.," October, vol. 1.1, no. c, pp. 1–21, 2011.

[9] J. F. Manwell, J. G. Mcgowan, and A. L. Rogers, "Wind Energy Explained Theory, Design and Application Second Edition," in Wiley, 2010, pp. 328–329.

[10] M. A. Yurdusev, R. Ata, and N. S. Çetin, "Assessment of optimum tip speed ratio in wind turbines using artificial neural networks," Energy, vol. 31, no. 12, pp. 1817–1825, 2006.

[11] R. Gasch and J. Twele, "Wind Power Plants," in Wind Power Plants, 2011, pp. 49–51.

[12] D. Marten, M. Lennie, G. Pechlivanoglou, C. N. Nayeri, and C. O. Paschereit, "Implementation, Optimization and Validation of a Nonlinear Lifting Line Free Vortex Wake Module Within the Wind Turbine Simulation Code QBlade," Vol. 9 Oil Gas Appl. Supercrit. CO2 Power Cycles; Wind Energy, no. December, p. V009T46A019, 2015.

[13] D. Marten, "QBlade v0.95 Guidelines for Lifting Line Free Vortex Wake Simulations," no. June, 2016.

APPENDIX

Table-3: Load characteristics of blade design

Element	r	dr	Chord	a	β	V	cl	cd	lift force	dfx	dfθ
1	1.4	1.4	3	0.317	45.94	7.61	1.221	0.095	60.96	423.9	350.8
2	2.8	1.4	4.1	0.408	59.04	8.90	1.221	0.095	83.45	921.4	459.4
3	4.2	1.4	3.93	0.441	66.55	10.8	1.221	0.095	124.5	1392.5	479.3
4	5.6	1.4	2.954	0.386	70.1	14.0	1.221	0.095	207.1	1775.1	487.9
5	7	1.4	2.363	0.363	73.289	17.16	1.221	0.095	310.1	2154.7	468.2
6	8.4	1.4	1.969	0.351	75.70	20.34	1.221	0.095	435.3	2541.2	441.1

7	9.8	1.4	1.688	0.345	77.565	23.54	1.221	0.095	583.2	2933.5	411.5
8	11.2	1.4	1.477	0.342	79.02	26.77	1.221	0.095	753.99	3329.3	380.9
9	12.6	1.4	1.312	0.339	80.18	30.01	1.221	0.095	948.14	3726.8	349.8
10	14	1.4	1.1816	0.338	81.13	33.26	1.221	0.095	1164.2	4127.3	318.7
11	15.4	1.4	1.074	0.337	81.9	36.52	1.221	0.095	1403.96	4528.1	287.3
12	16.8	1.4	0.984	0.336	82.57	39.80	1.221	0.095	1666.98	4929.1	255.9
13	18.2	1.4	0.908	0.335	83.13	43.08	1.221	0.095	1952.85	5330.9	224.5
14	19.6	1.4	0.844	0.335	83.62	46.34	1.221	0.095	2259.48	5735.0	193.2
15	21	1.4	0.787	0.335	84.04	49.63	1.221	0.095	2592.24	6136.6	161.6
16	22.4	1.4	0.7385	0.335	84.40	52.89	1.221	0.095	2944.22	6541.3	130.3
17	23.8	1.4	0.695	0.334	84.73	56.18	1.221	0.095	3321.08	6944.6	98.8
18	25.2	1.4	0.656	0.334	85.02	59.47	1.221	0.095	3722.27	7347.2	67.3
19	26.6	1.4	0.621	0.334	85.28	62.78	1.221	0.095	4147.25	7749.6	35.7
20	28	1.4	0.5908	0.334	85.519	66.03	1.221	0.095	4587.85	8156.0	4.4
TOTAL									33269.36	86725.03	5607.5